Full-potential KKR calculations for vacancies in Al: Screening effect and many-body interactions

T. Hoshino,[1] M. Asato,[2] R. Zeller,[3] and P. H. Dederichs[3]
[1]*Department of Applied Physics, Faculty of Engineering, Shizuoka University, Hamamatsu 432-8561, Japan*
[2]*Department of General Education, Tokyo Metropolitan College of Technology, Shinagawa-ku, Tokyo 140-0011, Japan*
[3]*Institut für Festkörperforschung, Forschungszentrum Jülich, D-52425 Jülich, Germany*
(Received 7 January 2004; revised manuscript received 3 May 2004; published 30 September 2004)

We give *ab initio* calculations for vacancies in Al. The calculations are based on the generalized-gradient approximation in the density-functional theory and employ the all-electron full-potential Korringa-Kohn-Rostoker Green's function method for point defects, which guarantees the correct embedding of the cluster of point defects in an otherwise perfect crystal. First, we confirm the recent calculated results of Carling *et al.* [Phys. Rev. Lett. **85**, 3862 (2000)], i.e., repulsion of the first-nearest-neighbor (1NN) divacancy in Al, and elucidate quantitatively the micromechanism of repulsion. Using the calculated results for vacancy formation energies and divacancy binding energies in Na, Mg, Al, and Si of face-centered-cubic, we show that the single vacancy in nearly free-electron systems becomes very stable with increasing free-electron density, due to the screening effect, and that the formation of divacancy destroys the stable electron distribution around the single vacancy, resulting in a repulsion of two vacancies on 1NN sites, so that the 1NN divacancy is unstable. Second, we show that the cluster expansion converges rapidly for the binding energies of vacancy agglomerates in Al. The binding energy of 13 vacancies consisting of a central vacancy and its 12 nearest neighbors, is reproduced within the error of 0.002 eV per vacancy, if many-body interaction energies up to the four-body terms are taken into account in the cluster expansion, being compared with the average error (>0.1 eV) of the glue models which are very often used to provide interatomic potentials for computer simulations. For the cluster expansion of the binding energies of impurities, we get the same convergence as that obtained for vacancies. Thus, the present cluster-expansion approach for the binding energies of agglomerates of vacancies and impurities in Al may provide accurate data to construct the interaction-parameter model for computer simulations which are strongly requested to study the dynamical process in the initial stage of the formation of the so-called Guinier-Preston zones of low-concentrated Al-based alloys such as $Al_{1-c}X_c$ (X=Cu, Zn; $c<0.05$).

DOI: 10.1103/PhysRevB.70.094118 PACS number(s): 71.15.Mb, 71.15.Nc

I. INTRODUCTION

Ab initio calculations based on the density-functional theory provide accurate data of materials properties and are expected to play an important role for material design. We have shown that the full-potential Korringa-Kohn-Rostoker (FPKKR) Green's function method for point defects, developed by the Jülich group,[1] combined with the generalized-gradient approximation of Perdew and Wang of the density-functional theory (PW91-GGA),[2] reproduce accurately the point-defect energies as well as the bulk properties of metals. For example, the equilibrium lattice parameters, bulk moduli, and monovacancy formation energies of elemental face-centered-cube (fcc) and body-centered-cubic (bcc) metals Li-Au are reproduced, respectively, within the errors of 1%, 10%, and 10% of the experimental values:[3] the generalized-gradient approximation (GGA) corrects the deficiency of the local-spin-density approximation (LSDA) of the density-functional theory, such as the underestimation of the equilibrium lattice parameter and the overestimation of the bulk modulus and monovacancy formation energy. The advantage of the Green's function method is that due to the introduction of the host Green's function, the embedding of point defects in an otherwise ideal crystal is described correctly, differently from the usual supercell and cluster calculations. It is noted that although the potential perturbation due to the defects is localized in the vicinity of the defects, the change of the wave functions due to the defects is delocalized over the whole space.[3,4] The practical advantage in using the Green's function method is to exploit this short-range nature of the defect potential. For example, in order to obtain the accurate and converged total energy of the defects in fcc metals, it is enough to redetermine self-consistently only the potentials of the defects and their nearest-neighboring host atoms, if the total energy change due to the perturbed wave functions over the infinite space is correctly evaluated by using the Lloyd's formula.[4] This is a big advantage of Green's function calculations, compared with the supercell and cluster calculations where all potentials must be recalculated in each iteration cycle. The energetics of point defects in complex periodic systems can be calculated by the present GGA-FPKKR method, because it allows one to calculate the electronic structure of complex periodic systems with a large number of atoms per unit cell by the screened FPKKR band structure calculation method.[5] The important advantage of the screened FPKKR band structure calculation method is the exploitation of the freedom in the choice of the reference system related to the real bulk system through the Dyson equation. Instead of a free-electron system the screened FPKKR method applies a reference system with repulsive potentials, leading to short-ranged structure constants which substantially simplify the numerical calculations as discussed by Zeller.[5] Thus at the present stage the GGA-FPKKR method is a most useful and accurate *ab initio*

method for the electronic structure of materials. Recently the measured temperature dependence of solid solubility limit of impurities in metals has also been reproduced accurately by the free-energy calculations based on the present GGA-FPKKR method combined with the cluster variation method.[6]

Using the *ab initio* pseudopotential approach combined with the supercell approximation, Carling *et al.* recently found that the first-nearest-neighbor (1NN) divacancy in Al is energetically unstable (repulsion of 1NN divacancy, positive values of divacancy binding energies) against two isolated monovacancies:[7] the GGA results (0.08 eV) is almost the same as the LDA result (0.07 eV). The result is in contrast to the commonly accepted interpretation of the experimental data on the non-Arrhenius temperature dependence of the vacancy concentration, in terms of the monovacancy-divacancy model where the interaction of a divacancy is assumed to be attractive due to the decrease of the number of the dangling bonds.[8] Using the molecular-dynamics (MD) simulations, however, Carling *et al*. showed in Ref. 7 that the non-Arrhenius temperature dependence of the vacancy concentration can arise from anharmonic atomic vibrations; the temperature dependence of the measured vacancy concentration can be explained without the presence of divacancies. Following the work of Carling *et al.* Uesugi *et al.*[9] also carried out the LDA-pseudopotential-supercell calculations for the divacancy binding energies in Al and obtained the repulsion for the 1NN (0.05 eV), which is similar to the local density approximation (LDA) and GGA values (0.07 eV, 0.08 eV) obtained by Carling *et al.* For the second-nearest-neighbor binding energy Uesugi *et al.* obtained the attraction (−0.04 eV, LDA), which is slightly different from the LDA and GGA values (−0.005 and −0.004 eV, very weak attraction) of Carling *et al.* Uesugi *et al.* discussed that larger supercells and larger **k** point numbers than those used in Ref. 7 are necessary to obtain converged numerical results, especially, for two vacancies on more distant neighboring sites. The FPKKR calculations for point defects are free of such convergence problems since they are not based on a supercell approach. The **k** summation is only needed once to calculate the structure Green's function matrix of pure fcc-Al (once per host), being needed for solving the Dyson equation of the impurity problem. The structure Green's function can be easily and accurately obtained by the bulk calculation of one atom per unit cell, therefore, a large number of **k** points poses no problem.

The aim of the present work is twofold. In Sec. II, we confirm the repulsion of the 1NN divacancy in Al and elucidate quantitatively its physical origin. The present GGA-FPKKR calculations show that the repulsion of the divacancy occurs in high-density free electron metals. In the present calculations we neglect the relaxation effects around vacancies.[10] However, it is noted that the present results do not change very much by the inclusion of the lattice relaxation effects because the earlier-mentioned supercell calculations[9,11] show the negligible contribution (0.004 eV, repulsion) to the binding energy of a divacancy, due to the cancellation of both the relaxation effects in the monovacancy and divacancy. We also discuss the limitations of the pair-potential model and the glue models,[12,13] both of them predict an attraction for the interaction between the nearest-neighboring vacancies in Al. In Sec. III, we show that the binding energies of agglomerates of vacancies and impurities in Al can be reproduced very well by the low-order many-body interaction energies (MBIEs) in the cluster expansion,[6] for example, up to three-body terms or four-body terms. Thus, the present cluster-expansion approach, based on the impurity calculations, may provide accurate data to construct an interaction-parameter model for computer simulations for the low-concentrated alloys, where the minor constituents of the elements are considered as impurities. In Sec. IV, we give a summary and discuss the possiblity of the present cluster-expansion approach to construct the interaction-parameter model for comuter simulations, which are needed to study the dynamical process in the initial stage of the formation of the Guinier-Preston (GP) zones for the low-concentrated Al alloys, such as $Al_{1-c}X_c$ ($X=Cu,Zn; c<0.05$).[14,15]

Here it may be necessary to discuss the differences between the present approach and the Connolly-Williams approach,[16,17] both of which calculate MBIEs in alloys by using the cluster expansion. The present approach, while restricted to the dilute limit, considers only atomic configurations, the energy differences of which define uniquely the many-body interactions. The MBIEs are determined successively from low-order to high-order interactions[6] and are independent of concentration. The Connolly-Williams approach also determines the MBIEs from different atomic configurations, but the results of the supercell calculations with many different configurations in the unit cell are fitted by models containing MBIEs. The best fit obtained by the smallest number of parameters determines the optional model for the interactions, which can therefore not be determined uniquely. It is also obvious that in order to obtain the MBIEs of point defects (dilute limit properties), the Connolly-Williams approach needs a large size of supercell, where the false interactions between point defects in the nearest-neighboring unit cells can be neglected. The interactions between the point defects may be longer than the region of the potential perturbation of defects, as discussed above. For example, the Nb-Nb interaction in Ag is long-ranged and is as large as −0.04 eV for the eighth neighbors:[6] it may be impossible to calculate accurately these long-ranged interactions by supercell calculations. These false interactions due to the defects in the neighboring unit cells may affect all atoms in the central unit cell, resulting in errors of the MBIEs.

On the other hand, the MBIEs obtained by the present approach, being accurate for a dilute limit, may become wrong with the increase of concentration of solute atoms. However, we have recently shown that for the concentration lower than ~10%, the concentration dependence of vacancy formation energies is accurately calculated by the present calculations combined with the direct configuration averaging.[18,19] Thus, we believe that in the same way the concentration dependence of MBIEs may also be calculated accurately for the low-concentrated alloys such as $Al_{1-c}X_c$ ($X=Cu,Zn; c<0.05$).

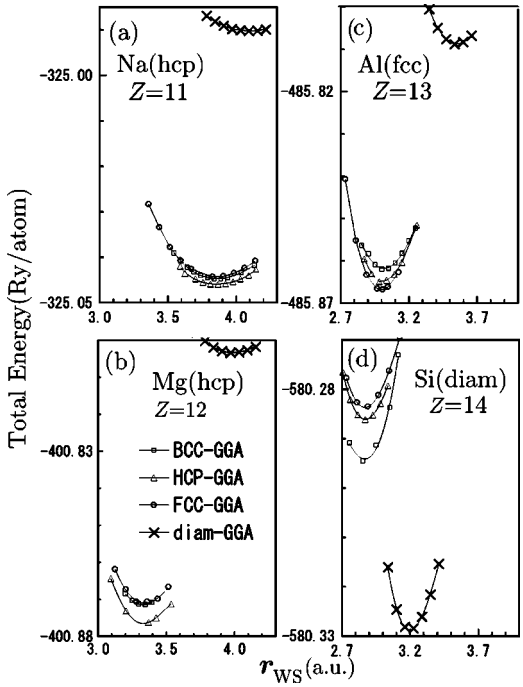

FIG. 1. PW91-GGA results for Wigner-Seitz radius dependence of total energies of (a) Na, (b) Mg, (c) Al, and (d) Al, for hcp, fcc, bcc, and diamond structures. See text for details.

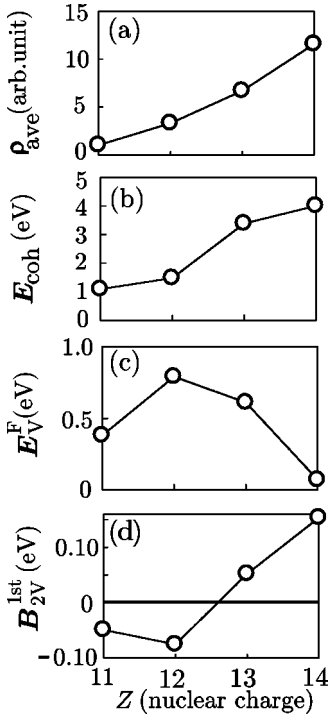

FIG. 2. (a) Average bulk-electron-density, (b) PW91-GGA results for cohesive energies, (c) monovacancy formation energies, and (d) binding energies of two vacancies, for Na ($Z=12$), Mg ($Z=13$), Al ($Z=13$), and Si ($Z=14$) of *fcc structure*. See text for details.

II. BINDING ENERGIES OF VACANCIES IN AL

In Sec. II A, we show that the present all-electron GGA-FPKKR calculations reproduce very well the repulsion of a 1NN divacancy in Al, which was obtained by the *ab initio* pseudopotential-supercell calculations. By examining the screening effect due to the free electrons, we elucidate the micromechanism of the repulsion. The long-ranged interaction energies of a divacancy in Al are also shown up to the eighth neighbor. In Sec. II B, we discuss the limitations of the pair-potential model and the glue models,[12,13] both of which predict an attraction of a 1NN divacancy in Al.

A. Divacancy binding energies in Al

In order to clarify the free-electron-density dependence of the screening effect, we carried out calculations for vacancies in Na, Mg, Al, and Si of *fcc structure*: the bulk electron-density increases from Na to Si by a factor of 10. It is noted that the measured ground-state atomic structures are, respectively, hexagonal-close-packed (hcp), hcp, fcc, diamond for Na, Mg, Al, and Si,[20] all of which are reproduced by the present total-energy calculations based on the screened GGA-FPKKR band structure method, as seen in Fig. 1: the calculated results of lattice parameters and cohesive energies agree with the experimental results, respectively, within the errors of 1% and 2%. Figure 2 shows the calculated results for vacancies in Na, Mg, Al, and Si of *fcc structure*, using the GGA equilibrium lattice constants (see Fig. 1): (a) average free-electron densities (ρ_{ave}), (b) cohesive energies (E_{coh}), (c) monovacancy formation energies (E_V^{F}), and (d) 1NN divacancy binding energies (B_{2V}^{1st}). The calculations for the structure constants were carried out by use of 891 symmetry inequivalent **k** points and the highest angular momentum $l_{\max}=4$. The details of the calculations for defect systems are discussed in Refs. 3 and 4. It is noted that E_V^{F} shows the energy loss caused by the formation of a vacancy. Positive values of B_{2V}^{1st} mean repulsion of a divacancy. The calculated results are summarized as follows.

(1) E_V^F [Fig. 2(c)] decreases rapidly with increasing free-electron-density [Fig. 2(a)] for Mg-Si: E_V^{F} is almost zero for fcc-Si.

(2) B_{2V}^{1st} [Fig. 2(d)] are negative (attraction) for Na and Mg, while positive (repulsion) for Al and Si. B_{2V}^{1st} increases with the free-electron-density for Mg-Si. The present GGA value (0.06 eV) for B_{2V}^{1st} agrees well with the LDA values (0.07 eV[7] and 0.05 eV[9]) and the GGA value (0.08 eV[7]), obtained by the pseudopotential-supercell calculations. The present value −0.007 eV for B_{2V}^{2nd} corresponds to the LDA values (−0.005 eV[7] and −0.04 eV[9]) and the GGA value (−0.004 eV) obtained by the pseudopotential-supercell approximation. The interaction of a divacancy is long-ranged, as shown in Fig. 3.

(3) The increase of B_{2V}^{1st} [Fig. 2(d)] for Mg-Si is correlated with the decrease of E_V^{F} [Fig. 2(c)].

(4) The ratios of E_V^F/E_{coh} and $B_{2V}^{\mathrm{1st}}/E_V^F$ (Table I) are, respectively, very different from the values (1 and $-1/6$) obtained by a simple pair-potential model.

We may conclude from the results (1), (2), and (3) that in the high-density-free-electron systems the formation of

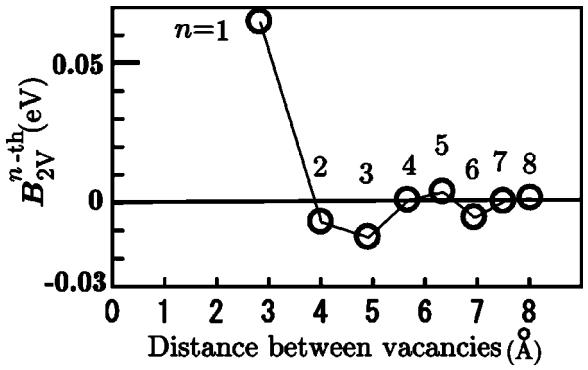

FIG. 3. Distance dependence of divacancy binding energies up to the eighth neighbor.

monovacancies becomes, due to the so-called screening effect, a very favorable mechanism and that the formation of a 1NN divacancy destroys this favorable configuration, leading to a repulsion of the divacancy. The importance of the screening effect in Al is also demonstrated by the electron redistribution around a vacancy, shown by the calculations of Carling *et al.*[7] and Polatoglou *et al.*:[21] the vacancy induces an accumulation of charge between the 12 nearest-neighboring atoms of the monovacancy, against the decrease of the coordination number of those atoms. This effect involves the vacancy and the two of its nearest neighbors and thus basically represents a three-body interaction. From a chemical-bond picture, it means that the free electrons around a vacancy are redistributed to strengthen the back bonds around a vacancy: the resultant energy gain due to the backbond strengthening nearly overcomes the energy loss due to the creation of dangling bonds. The earlier-mentioned mechanism may not work for vacancies in diamond-Si because the bulk electrons of diamond-Si [ground state of Si, Fig. 1(d)] are not free-electron like. On the other hand, the present mechanism may be valid for vacancies in hcp-Na and hcp-Mg because of the similarity of fcc and hcp structures (the same nearest-neighbor atomic configuration) and the small total-energy differences between them, as seen in Figs. 1(a) and 1(b).

TABLE I. Calculated results (in electron-volts) for Na, Mg, Al, and Si of *fcc structure*: cohesive energies (E_{coh}), monovacancy formation energies (E_V^{F}), first-nearest-neighbor divacancy binding energies (B_{2V}^{1st}), ratios of E_V^{F} with E_{coh}, and ratios of $B_{2V}^{1\text{st}}$ with E_V^{F}. According to the simple pair-potential model, for fcc the ratios E_V^F/E_{coh} and $B_{2V}^{1\text{st}}/E_V^F$ are, 1 and $-1/6$ (fcc), respectively. See text for details.

Element	Na	Mg	Al	Si
E_{coh}	1.09	1.48	3.39	4.01
E_V^{F}	0.38	0.79	0.61	0.07
$B_{2V}^{1\text{st}}$	−0.05	−0.08	0.06	0.15
E_V^F/E_{coh}	0.35	0.53	0.18	0.02
$B_{2V}^{1\text{st}}/E_V^F$	−0.13	−0.10	0.08	2.14

B. Pair-potential model and glue models for binding energies

In this section we discuss the limitations of pair-potential model and the glue models,[12,13] both of which predicts an attraction of the 1NN divacancy, very differently from the *ab initio* results.

First, we discuss the limitations of the pair-potential model for the point-defect energies in Al, where the total energy is written as a sum of the pair potentials. The important failures of the pair-potential model are well known: (1) the vacancy formation energy is equal to the cohesive energy and (2) the binding energy of the 1NN divacancy is $-1/6$ of the vacancy formation energy. The differences of the present calculated results with the results obtained from the pair-potential model become large for the high-density free-electron systems: the errors of E_V^F and $B_{2V}^{1\text{st}}$ in Al are, respectively, as large as 2.68(=3.39−0.61) eV and −0.16(=−0.10 −0.06) eV and the errors become much larger for fcc-Si due to the even higher free-electron density, as shown in Table I.

We now discuss that the glue models also do not reproduce accurately the binding energies of vacancy agglomerates. The glue models include the embedded-atom-method (EAM) because both the models have the same mathematical form

$$E = \sum_i E^i, \tag{1}$$

$$E^i = \sum_{j \neq i} \phi(\mathbf{r}_{ij}) + U(n^i), \tag{2}$$

$$n^i = \sum_{j \neq i} \rho(\mathbf{r}_{ij}), \tag{3}$$

where E is the total energy, $\phi(\mathbf{r}_{ij})$ is the two-body central potential between atoms i and j, $\rho(\mathbf{r}_{ij})$ is the electron density at atom i due to all other atoms, $U(n^i)$ is associated with the many-body potentials beyond the two-body potential ϕ.[12,13] According to Johnson,[22] the binding energies of divacancy, trivacancy, and tetravacancy, obtained by the EAM are almost the same as those obtained by the simple pair-potential model which takes into account only the number of dangling bonds. It is noted that the correct description of the backbond-strength dependence of the local environment needs the accurate estimation for the MBIEs of a vacancy with its nearest-neighboring atoms, as discussed by Moriarty[23] and Tersoff.[24] The backbond strengthening due to the formation of vacancies may be one of the bonding effects beyond the glue models. The accurate estimation for binding energies $B_{nV}^{1\text{st}}$ (n vacancies of first neighbors) of vacancy agglomerates in Al needs not only the environment dependence of coordination number, but also the environment dependence of the atomic charges [$\rho(\mathbf{r}_{ij})$ in Eq. (3)]. It is noted that the glue models include only the environment dependence of the coordination number because the environment dependence is described by the superposition of atomic charges which are not dependent on the environment.

TABLE II. Calculated results (in electron-volts) for monovacancy formation energies (E_V^F) and binding energies of $n(=2-13)$ vacancies of first neighbors (B_{nV}) in Al, based on the two kinds of glue model and the GGA-FPKKR method. See text for the glue models.

Method	Glue 1[a]	Glue 2[b]	GGA-FPKKR
E_V^F	1.41	0.48	0.61
B_{2V}	−0.20	−0.06	0.06
B_{3V}	−0.70	−0.14	0.10
B_{4V}	−1.30	−0.28	0.01
B_{13V}	−10.53	−4.32	−0.95

The limitations of the glue models for the different coordination numbers (0–12) were already discussed by Robertson *et al.*,[13] testing many different (>25) glue models: none gives a root-mean-square error less than 0.1 eV and the individual energy errors range from −0.3 to 0.3 eV per atom. These errors may contribute to the bonding effects beyond the glue formalism. Table II lists the results of B_{nV}^{1st} (a central and its nearest 12 neighbors for $n=13$), obtained by the two kinds of glue models, made by Robertson *et al.*[13] The database of 171 total energies, constructed by *ab initio* calculations based on the LSDA in the density functional formalism, were used to determine the parameters of the models, one of which (glue 1 in Table II) takes into account only the nearest neighbor interaction, while the other (glue 2 in Table II) takes into account the interactions beyond the nearest-neighbor. The parameters in the models and the results for B_{nV}^{1st} are very different, as shown in Table II. This sensitivity is a general character for the glue models, as discussed by Robertson *et al.*[13] It may be concluded from these results that the simple glue models[13] predict attraction for interactions of vacancies, in the same way as the pair-potential model, and the errors for B_{nV}^{1st} become larger with n, compared with the present GGA-FPKKR results. It is noted that the differences between B_{nV}^{1st}'s obtained by the LDA and GGA calculations are very small, compared with the differences between B_{nV}^{1st}'s obtained by the GGA calculations and the glue models.

III. CLUSTER-EXPANSION APPROACH FOR THE BINDING ENERGIES

In Sec. III A, we discuss the convergence of the cluster expansion for the binding energies of the agglomerates of (2–6) vacancies and show that the binding energies of (4–6) vacancies may be reproduced very well by the low-order MBIEs in the cluster expansion up to the three-body term, all of which are obtained from the calculated results for two and three vacancies, because the many-body interaction energies beyond the three-body term are very small. In Sec. III B, we show the convergence of the cluster expansion for the binding energies of the larger agglomerates of 13 vacancies and impurities (Cu and Zn).

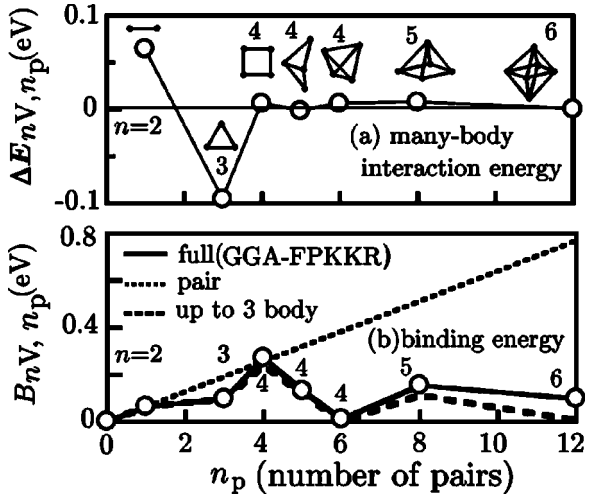

FIG. 4. (a) Many-body interaction energies ($\Delta E_{nV,n_p}$) and (b) binding energies (B_{nV,n_p}), as a function of a number of vacancies $n(=2-6)$ and a number of pairs $n_p(=2-12)$. The results obtained by the pair (two-body) interaction model [dotted line in Fig. 4(b)] includes only the nearest-neighbor interaction energy, while the interaction model up to the three-body term [broken line in Fig. 4(b)] the pair interaction energies up to second neighbor and the three-body interaction energy of first-neighbors. See text for details.

A. Vacancies

We use the more accurate expression for the binding energies of vacancies (B_{nV,n_p}), differently from the definition (B_{nV}) used in Sec. II, which classifies the different shapes for the same number n of vacancies by the number n_p of nearest-neighboring pairs. The MBIEs ($\Delta E_{nV,n_p}$) are also expressed in the same way. We consider the pair ($n=2$ and $n_p=1$), triangle ($n=3$ and $n_p=3$), square ($n=4$ and $n_p=4$), bent rhombus ($n=4$ and $n_p=5$), tetrahedron ($n=4$ and $n_p=6$), pyramid ($n=5, n_p=8$) and octahedron ($n=6$ and $n_p=12$) of first-neighbors, as shown in Fig. 4(a). Figure 4 shows (a) $\Delta E_{nV,n_p}$ and (b) B_{nV,n_p}, as a function of $n(=2-6)$ and $n_p(=1-12)$. It is noted that the MBIEs beyond the three particles are very small. Thus, we can expect that the B_{nV,n_p} for large n are reproduced by the MBIEs up to the three-body term. In fact we can see in Fig. 4(b) that B_{nV,n_p} are reproduced very well by the cluster expansion up to the three-body term. The error for an octahedron of vacancies ($n=6$ and $n_p=12$) is ~0.02 eV per vacancy. If the two-body interaction of second-neighbor and the three-body interaction of a triangle with one second neighbor are taken into account, the error becomes as small as ~0.01 eV per vacancy. On the other hand, the error of the pair-potential model of nearest-neighbor becomes larger with n and is larger than 0.1 eV per vacancy, for an octahedron of vacancies, as shown in Fig. 4(b).

We note that the binding energy of 13 vacancies, as an example of the larger agglomerates of vacancies, is very well (the error of 0.002 eV per vacancy) reproduced by the cluster expansion including up to the three-body terms or the four-body terms, as discussed in the next subsection.

TABLE III. Calculated results (in electron-volts) for binding energies of 13 vacancies and impurities. The cluster-expansion results including up to the four-body interaction energies are given together with the exact GGA-FPKKR results. See text for details.

Up to n-body	$n=2$	$n=3$	$n=4$	Exact
Vacancy_{13}	1.90	−0.95	−0.92	−0.95
Cu_{13}	1.04	1.96	1.92	1.94
Zn_{13}	−0.63	−0.53	−0.50	−0.49

B. Impurities

We examined the cluster expansion for the binding energies of Cu and Zn agglomerates in Al. The calculated results for a impurity cluster consisting of a central impurity and its 12 nearest-neighbors, are shown in Table III. The cluster expansion includes the two-body interaction energies up to the third-neighbors, and the three-body interaction energies with one second-neighbor and two first-neighbors, together with the MBIEs up to the three kinds of four-body terms, shown in Fig. 4(a). We can obtain the same convergence as that obtained for 13 vacancies: the error is 0.002 eV per vacancy or impurity, compared with the average error 0.1 eV of the glue models.[13]

As shown earlier, the inclusion of the three-body interaction is most important for a reliable estimate of the binding energies.

IV. SUMMARY AND FUTURE PROBLEM

First, we have confirmed the repulsion of the 1NN divacancy in Al and elucidated quantitatively the micromechanism of repulsion. The calculations are based on the generalized-gradient approximation[2] in the density-functional formalism and the FPKKR method[1,3,4] which treats the correct embedding of the cluster of point defects in an otherwise Al crystal. The limitation of the pair-potential model and the glue models, both of which predict an attraction of the 1NN divacancy in Al, has also been discussed.

Second, we have examined the convergence of the cluster expansion of the binding energies of agglomerates of vacancies and impurities. It was shown that the cluster expansion converges rapidly and the binding energies of 13 vacancies and 13 impurities (Cu or Zn as impurities) are reproduced within the error of 0.002 eV per vacancy or impurity, if the MBIEs up to the four-body terms are taken into account in the cluster expansion.

At the end of the paper, we want to discuss the usefulness of the present cluster-expansion approach to constitute the interaction-parameter model for computer simulations which are needed to study the dynamical process in the initial stage of the formation of GP zones of low-concentrated Al-based alloys. Recently many experiments have been carried out to investigate the dynamical process in the initial stage of the formation of GP zones. The primary motivation for these works is the desirable technological properties of many these alloys, for example, their light weight and high strength. For example, Sato *et al.*[14,15] showed experimentally that a small amount of Mg markedly accelerates the GP zone formation of $\text{Al}_{1-c}\text{Cu}_c$ ($c<0.05$) and enhances age-hardening. Using the Monte-Carlo computer simulation with the simple pair-interaction model, they also discussed a physical picture: the Mg/Cu/vacancy clusters formed in the initial stage act as effective nucleation sites for GP zones and resultantly accelerate the formation of fine and high-density clusters, which increases the strengthening due to the age hardening. In order to examine this physical picture we need an accurate interaction-parameter model beyond the pair-potential model. We believe that the present cluster expansion approach may be useful for the construction of the interaction-parameter model for the low-concentrated Al-based alloys such as $\text{Al}_{1-c}\text{X}_c$ ($\text{X}=\text{Cu, Zn}$; $c<0.05$) because the solute X atoms of low concentration may be considered as impurities: the present cluster-expansion approach provides the accurate data for a dilute limit and the concentration dependence of MBIEs in the low-concentrated alloys may be calculated by the present method combined with the direct-configurational averaging, as shown in Refs. 18 and 19. In addition to the high accuracy and economical efficiency of the present approach, there are some other advantages. We found that the sign and magnitude of the three-body interaction energies of first neighbors are correlated to the shapes of the GP zones, just as the sign and magnitude of the two-body interaction energies are connected with the different types of phase diagrems of binary alloys, such as segregation, solid solution, and orderering.[6,25] For example, three-body interaction energies of Cu impurities and Zn impurities are, respectively, positive (0.03 eV, repulsion) and zero, which correspond to the (001) disk and the spherical shape of GP zones, respectively; it is noted that there is no triangle cluster of first-neighbors in the (001) layer of fcc structure. The micromechanisms of structural stability of small clusters may be elucidated, as discussed in Refs. 25 and 26; for example, the Cu/Mg/vacancy cluster may become stable by both the attractive interactions of Cu-Mg and Mg-vacancy. It is also an advantage of the present method to treat easily the effect of quenched-in excess vacancies and additional elements of solutes: the systems may easily be studied as an impurity problem. The details will be published elsewhwere.[27]

It is obvious that the lattice relaxation effects become important for clusters of solute atoms of large atomic-radius misfit, compared with the host atom.[10] The modeling of the lattice relaxation energies, interpolating the *ab initio* results, may be needed to complete the accurate interaction-parameter model for computer simulations, although this is a time-consuming and difficult problem.

ACKNOWLEDGMENT

The authors are grateful for the financial support of the Ministry of Culture, Science and Education (Grant No. 15074206).

[1] P. H. Dederichs, T. Hoshino, B. Drittler, K. Abraham, and R. Zeller, Physica B **172**, 203 (1991); P. H. Dederichs, B. Drittler, and R. Zeller, in *Application of Multiple Scattering Theory to Material Science*, MRS Symposia Proceedings No. 253, edited by W. H. Butler *et al.* (Materials Research Society, Pittsburgh, 1992), p. 185.

[2] J. P. Perdew, in *Electronic Structure of Solids '91*, edited by P. Ziesche and H. Eschrig (Akademie-Verlag, Berlin, 1991), p. 11; J. P. Perdew, J. A. Chevary, S. H. Vosko, K. A. Jackson, M. R. Pederson, D. J. Singh, and C. Fiolhais, Phys. Rev. B **46**, 6671 (1992).

[3] T. Hoshino, T. Mizuno, M. Asato, and H. Fukushima, Mater. Trans., JIM **42**, 2206 (2001); M. Asato, A. Settels, T. Hoshino, S. Blügel, T. Asada, R. Zeller, and P. H. Dederichs, Phys. Rev. B **60**, 5202 (1999).

[4] B. Drittler, M. Weinert, R. Zeller, and P. H. Dederichs, Phys. Rev. B **39**, 930 (1989).

[5] R. Zeller, Phys. Rev. B **55**, 9400 (1997); R. Zeller, M. Asato, T. Hoshino, J. Zabloudil, P. Weinberger, and P. H. Dederichs, Philos. Mag. B **78**, 417 (1998); T. Hoshino, M. Asato, K. Nakamura, R. Zeller, and P. H. Dederichs, J. Magn. Magn. Mater. **272–276**, 229 (2004).

[6] M. Asato, T. Mizuno, T. Hoshino, and H. Sawada, Mater. Trans., JIM **42**, 2216 (2001).

[7] K. Carling, G. Wahnström, T. R. Mattsson, A. E. Mattsson, N. Sandberg, and G. Grimvall, Phys. Rev. Lett. **85**, 3862 (2000).

[8] T. Hehenkamp, J. Phys. Chem. Solids **55**, 907 (1994).

[9] T. Uesugi, M. Kohyama, and K. Higashi, Phys. Rev. B **68**, 184103 (2003).

[10] N. Papanikolaou, R. Zeller, P. H. Dederichs, and N. Stefanou, Phys. Rev. B **55**, 4157 (1997); T. Hoshino, N. Papanikolaou, R. Zeller, P. H. Dederichs, M. Asato, T. Asada, and N. Stefanou, Comput. Mater. Sci. **14**, 56 (1999).

[11] T. Uesugi (private communication).

[12] *Many-Atom Interactions in Solids*, Springer Proceedings in Physics 48, edited by R. M. Nieminen *et al.* (Springer-Verlag, Berlin, 1990).

[13] I. J. Robertson, V. Heine, and M. C. Payne, Phys. Rev. Lett. **70**, 1944 (1993).

[14] S. Hirosawa, T. Sato, and A. Kamio, Mater. Sci. Eng., A **242**, 195 (1998).

[15] T. Sato, S. Hirosawa, K. Hirose, and T. Maeguchi, Metall. Mater. Trans. A **34**, 2745 (2003).

[16] J. W. Connolly and A. R. Williams, Phys. Rev. B **27**, 5169 (1983).

[17] J. M. Sanchez, F. Ducastelle, and G. Gratias, Physica A **128**, 334 (1984).

[18] M. Asato and T. Hoshino, J. Magn. Magn. Mater. **272–276**, 1372 (2004).

[19] H. Dreyssé, A. Bererra, L. T. Wille, and D. de Fontaine, Phys. Rev. B **39**, 2442 (1989); D. de Fontaine, *Solid State Physics*, edited by H. Ehrenreich and D. Turnbull (Academic Press, London, 1994), Vol. 47, p. 33; T. Hoshino and K. Masuda-Jindo, *Properties of Complex Inorganic Solids*, edited by A. Gonis *et al.* (Plenum Press, New York, 1997), p. 129.

[20] C. Kittel, *Introduction to Solid State Physics*, 7th ed. (Wiley, New York, 1996); M. M. Dacorogna and M. L. Cohen, Phys. Rev. B **34**, 4996 (1986); G. K. Straub and D. C. Wallace, Phys. Rev. B **3**, 1234 (1971).

[21] H. M. Polatoglou, M. Methfessel, and M. Scheffler, Phys. Rev. B **48**, 1877 (1993).

[22] R. A. Johnson, Phys. Rev. B **37**, 3924 (1988).

[23] J. A. Moriarty, in *Many-Atom Interactions in Solids*, Springer Proceedings in Physics 48, edited by R. M. Nieminen *et al.* (Springer-Verlag, Berlin, 1990), p. 158.

[24] J. Tersoff, Phys. Rev. Lett. **56**, 632 (1986).

[25] T. Hoshino, R. Zeller, P. H. Dederichs, and T. Asada, *Computational Physics as a New Frontier in Condensed Matter Research*, edited by H. Takayama *et al.* (Physical Society of Japan, Tokyo, 1995), p. 105.

[26] T. Hoshino, R. Zeller, and P. H. Dederichs, Phys. Rev. B **53**, 8971 (1996).

[27] T. Hoshino and F. Nakamura, a special issue of Journal of Metastable & Nanocrystalline Materials; F. Nakamura, T. Hoshino, K. Hirose, S. Hirosawa, and T. Sato (unpublished).